Construction and tribological properties of 2D heterojunction of g-C₃N₄/MoS₂ nanocomposites

G. X. Qiu[*], W. F. Hang, W .Li, G. G Tang
Changzhou Vocational Institute of Engineering, Changzhou, Jiangsu Province, 213164, PR China

2D/2D heterojunction of flower-like MoS_2 nanosheets anchored on g-C_3N_4 was fabricated through a facile hybridization approach, and systematically investigated by various characterization methods (e.g. XRD, SEM, TEM and XPS analysis). Furthermore, tribological properties of g-C_3N_4/MoS_2 composites containing with liquid paraffin were comparatively measured by UMT-2 multispecimen friction and wear tester, and various tribological variables including additive concentration, applied load and rotational speed were also investigated in details. Among all samples, 2%-g-C_3N_4/MoS_2 composites exhibit the minimal friction coefficient (~0.08), and the anti-wear performance is improved obviously. The improvement of tribological properties of the base oil is due to the synergistic effect of g-C_3N_4 and ultra-thin molybdenum disulfide nanosheets. This study provides a new idea for the design of two-dimensional layered composites with enhanced tribological properties of lubricating oil and matrix.

1. Introduction

Generally, friction and wear are ubiquitous and inevitable in modern society, which often cause energy and material consumption, and environmental pollution, and are the major causes of disastrous accident consequences. Nowadays, the wide application of lubrications has been regarded as one of the most effective and successful strategies for promoting tribological properties and service life of the facility[1-5]. Among them, liquid lubrication (e.g. water or oil) is the most age-old approach for minimizing friction and wear. Furthermore, with the addition of lubricant additives, such as commercial graphite and MoS_2, the friction-reducing and antiwear performance of traditional lubricating oil was significantly improved[6-10]. With progress in nanoscale science and technology, many inorganic nanoparticles have been introduced as ideal lubricant additives to optimize the traditional liquid-solid lubricating system because of their obvious anti-friction and anti-wear properties. Moreover, excellent nanoadditives should have appropriate size, shape, structure, high stability and mechanical features[11-15]. Thus, it is still one

---

of the biggest challenges to explore and develop new multifunctional nano-lubricants or nano-additives with high efficiency, low cost and environmental protection.

As we know, traditional lubricants represented by graphite and MoS_2 have been always extensive applied to anti-wear and antifriction because of their distinctive lamellar structure[16-18]. Many previous researches indicate nanosized lubricants usually exhibit better anti-wear property and friction-reducing efficiency than that of commercial lubricants. Compared to conventional lubricant additives, nanoparticles exhibit many advantages, such as the multiple possibilities of film formation on many different types of surfaces, durability and low volatility ,and withstand high temperature condition. Considering of this, graphene-like 2D materials (such as graphene, MoS_2, g-C_3N_4 and h-BN) have been widely regarded as the most promising of oil additives due to their weak van der Waals interlayer interactions and strong covalent intralayer interactions[19-22]. Among them, especially MoS_2 nanomaterials have shown great potential in the field of tribology because of its hexagonal lamellar structure, superior stability, thermal and mechanical performance. More importantly, MoS_2 has the sandwiched structure consisting of Mo atomic layer intercalated into two S atomic layers, which could slide easily on the friction interface, resulting in the lower friction coefficient between interfaces. Unfortunately, MoS_2 nanomaterials usually exhibit low dispersion in lubricating oil because of their high specific surface area, and serious aggregation and precipitation largely inherit their actual application in the field of lubricant and friction. Therefore, various modification strategies have been explored and developed to modify and optimize MoS_2 nanomaterials for promoting the tribological properties and dispersion in lubricating oils.

Generally, many previous researches indicate constructing MoS_2-incorporated nanocomposites can efficiently enhanced tribological properties and extend their various applications. Once MoS_2 coupled with other nanoparticles (such as TiO_2 particles, carbon nanotubes, graphene, and other transition metal dichalcogenides), MoS_2-based nanocomposites provide much more reinforcing and lubricating effects than that of single one. In recent years, another typical two-dimensional material (g-C_3N_4) has become an ideal candidate for green lubricant additives due to its excellent stability, dispersion, ultra-high hardness and graphite structure with weak van der Waals forces. Furthermore, the high chemical, thermal, and hydrothermal stability can also be beneficial for the design and construction of g-C_3N_4-based lubricant and additive. The synthesis and tribological performance of g-C_3N_4/TiO_2 hybrids as oil additives have been reported by Zhang et al. Still, there are few literatures on 2D/2D heterostructured g-C_3N_4/MoS_2 as lubricating oil additives.

Herein, the novel 2D/2D heterojunction of MoS_2 nanosheets grafted with g-C_3N_4 ultrathin nanosheets were constructed by an in-situ hydrothermal process, and its morphology, structure, and chemical composition were systematically characterized. Moreover, g-C_3N_4/MoS_2 composite are further used as additives in paraffin for the evaluation of lubrication properties by a UMT-2 ball-on-disc sliding tribometer. The results showed that the composite significantly improved the wear resistance of base oil. In addition, the tribological behavior and mechanism of g-C_3N_4/MoS_2 as lubricating additive were discussed in detail.

2. Experimental section

2.1. The preparation of g-C$_3$N$_4$

Graphitic g-C$_3$N$_4$ was roasted with urea as the precursor. The specific experimental method was as follows: 10 g urea was added to the crucible, and then roasted at 550 in muffle furnace for 2 h at a heating rate of 5/min. The synthesized yellow powder was washed with deionized water and anhydrous ethanol for several times, and finally dried at 60℃ for 12 h in vacuum to obtain the g-C$_3$N$_4$ lamellae structure.

2.2. Synthesis of g-C$_3$N$_4$/MoS$_2$ composites

MoS$_2$/g-C$_3$N$_4$ composite nanosheets were synthesized by a typical hydrothermal method. The experimental steps were as follows: the graphite powder prepared in 0.1g 5.4.1.1 was dispersed into 50 mL deionized water, then 0.725 g NH$_2$OH•HCl and 1.40 g CH$_4$N$_2$S were respectively dissolved in the above solution, and the pH of the solution was adjusted to about 6 with 2 mol/L HCl. After stirring the solution magnetically for 1 h, the solution was transferred to a 100 mL hydrothermal reaction kettle, which was placed in an oven and reacted at 180°C for 24 h, and then cooled naturally to room temperature. After centrifugation, the black products were washed with anhydrous ethanol and deionized water for several times. Finally, the samples were dried at 60℃ for 12 h under vacuum conditions to obtain hydrothermal synthesis samples.

2.3. Characterization

XRD analysis (Bruker-AXS, Germany), FT-IR spectra (Thermo Nicolet Model Nexus 470, America) and Raman (DXR-Thermo Scientific) were performed to analyze phase structure and chemical composition of the as-prepared nanomaterials. SEM technique (JEOL JXA-840A, Japan) and TEM (JEM-100CX II, Japan) were used to characterize their surface micromorphology and structure.

2.4. Tribological Test

In this work, a multispecimen friction and wear tester (UMT-2, USA) with ball-on-disk construction was used to evaluate the tribological properties of the oil mixtures contained with nano-additives. And liquid paraffin was used as the lubricating oil in the friction experiments. During experiments, the rotary velocity of steel ball is 100 rpm, and applied load is 5 N for 0.5 h at room temperature. Additionally, different adsorption variables including the additive concentration (0.5-5wt%), rotary velocity (100-500rpm), and applied load (5-30N) were also investigated. More importantly, all friction experiments were investigated three times, respectively. After that, the surface topography of the wear scar were analyzed by scanning electron microscope (SEM, HITACHI S-3400N, Japan) and non-contact optical 3D profilers (SMP, NT1100, Veeco WYKO, USA).

3. Results and discussion

The crystal phase composition and phase purity of the as-synthetized g-C$_3$N$_4$/MoS$_2$ hybrids were investigated by XRD analysis. As illustrated in Fig. 1a, two characteristic diffraction

peaks of pristine g-C$_3$N$_4$ located at 13.3° and 27.5° can be ascribed to (100) and (002) planes of g-C$_3$N$_4$ (JCPDF 87-1526), which were respectively related to the interplanar structural packing and interlayer stacking structure[23,24]. For the XRD spectrums of g-C$_3$N$_4$/MoS$_2$ nanosheets, the main phase were similar to MoS$_2$ (JCPDS Card No. 75-1539)[25-26]. However, no obvious peaks of g-C$_3$N$_4$ were obtained because of its low concentration of g-C$_3$N$_4$ in the composites. Moreover, the (002) plane at 14.2° with higher diffraction intensity indicated the formation of a well-stacked layered structure.
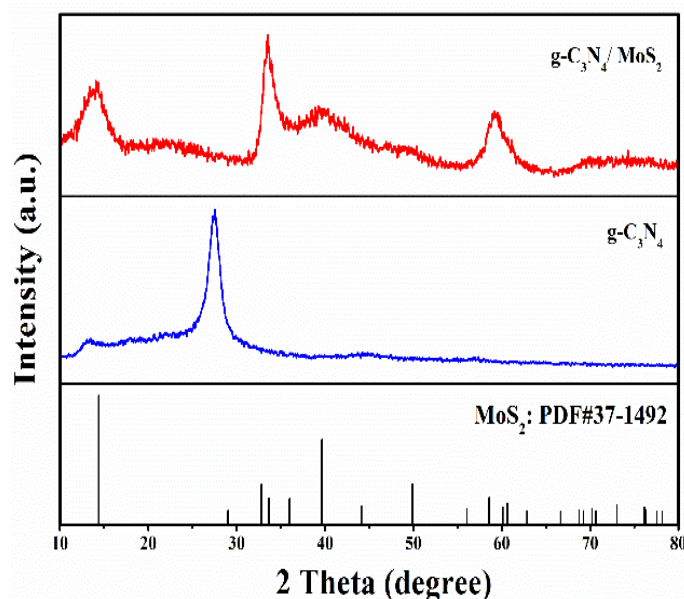
Fig. 1. XRD pattern of the as-preparedg-C$_3$N$_4$/MoS$_2$.

Further, XPS measurement was carried out to confirm the coexistence of MoS$_2$ and g-C$_3$N$_4$. As shown Fig. 2a, the XPS signals of C, N, Mo, and S elements were obtained in the survey spectra of g-C$_3$N$_4$/MoS$_2$. In Fig. 2b, two obvious peaks at 229.3 and 232.5 eV was according to Mo^{4+} oxidation state (Mo 3d$_{5/2}$ and3d$_{3/2}$). Obviously, the high-resolution C 1s spectrum (Fig. 2c) can be fitted with three characteristic band of C-C (284.6 eV), N-C=N (288.8 eV) and C=N (286.8 eV). And N 1s spectrum exhibits three peaks at 398.6, 399.3, and 401.2 eV as shown in Fig.2e, which signals corresponding to C-N=C, N-(C)$_3$, C-N-H groups, respectively. Furthermore, two pronounced peaks of S 2p located at 162.1 and 163.3 eV are assigned S 3d$_{5/2}$ and S3d$_{3/2}$, resulted in the presence of MoS$_2$(Fig. 2b).

The microstructure and morphologies of g-C$_3$N$_4$, MoS$_2$ and g-C$_3$N$_4$/MoS$_2$ composites were investigated by SEM and TEM. As observed from Fig. 3a, g-C$_3$N$_4$ possessed typical sheet-like structures, and MoS$_2$ is consisted of uniform flower-like sheets with average grain size around 100-200nm (Fig. 3b). After hydrothermal synthesis, g-C$_3$N$_4$/MoS$_2$ composites show the similar sheets-like structure of MoS$_2$ (Fig. 3c), while a large number of MoS$_2$ nanosheets were grown on the surface of sheets-like g-C$_3$N$_4$ with intimate interaction (Fig. 3c). Furthermore, characterized by HRTEM (Fig. 3d), MoS$_2$ nanosheets is consisted of several layer, and its interlayer distance is about 0.63 nm, according to the theoretical spacing for (002) planes of MoS$_2$. Thus, the SEM and

TEM images together with XRD and XPS spectra reveal the successful synthesis of g-C_3N_4/MoS_2 heterojunction.
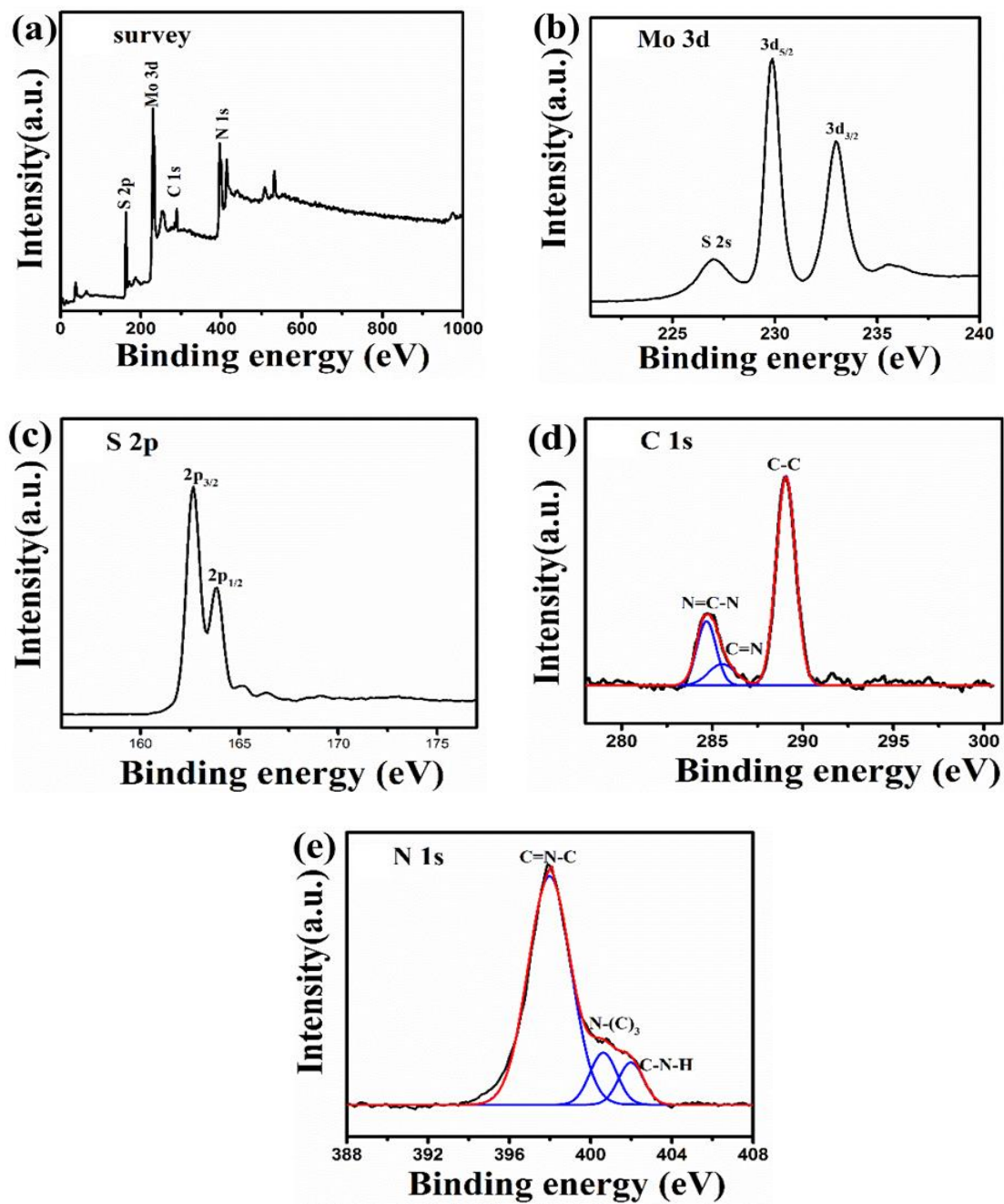

Fig. 2. XPS spectra of g-C$_3$N$_4$/MoS$_2$ composite: (a) survey spectrum, (b) Mo 3d, (c) S 2ps, (d) C 1s and (e) N 1s.
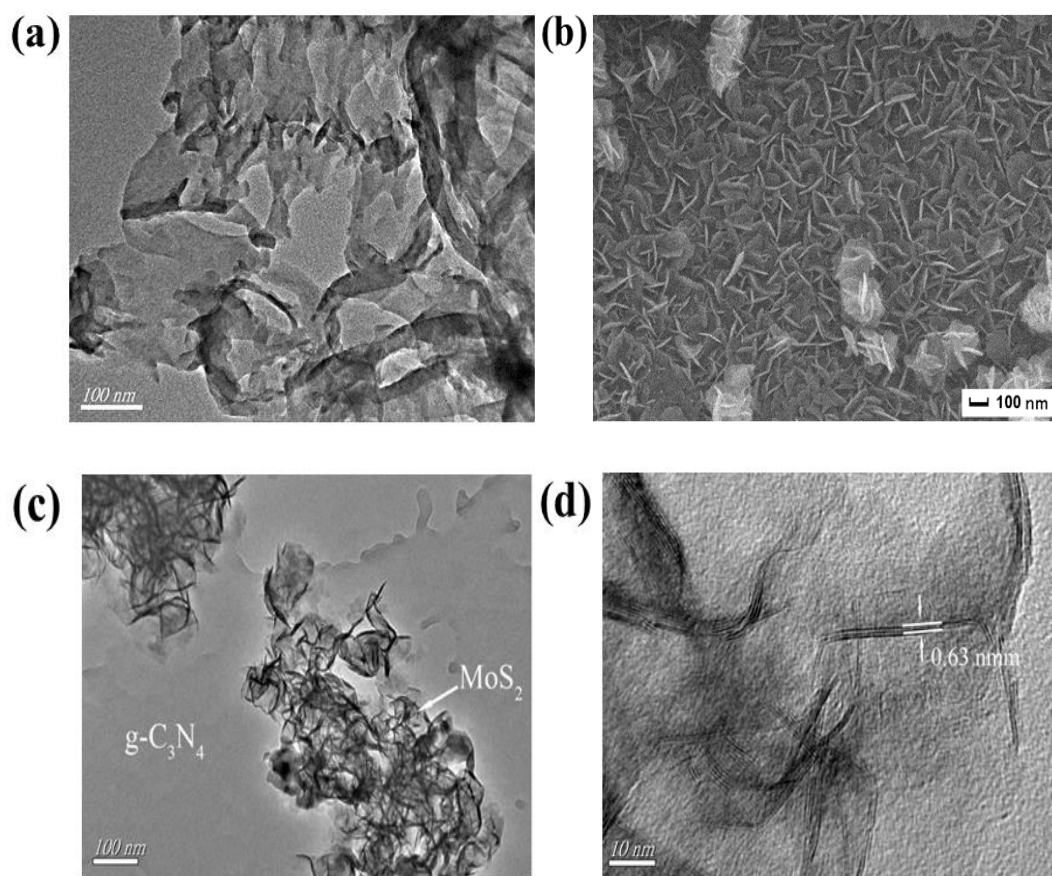
Fig. 3. SEM (a, b) images of the as-prepared g-C$_3$N$_4$ and MoS$_2$,TEM (c) and HRTEM (d) images of the as-prepared g-C$_3$N$_4$/MoS$_2$nanosheets.

Fig. 4a depicts the friction behavior of pure g-C$_3$N$_4$, MoS$_2$ and g-C$_3$N$_4$/MoS$_2$ in the paraffin oil. Obviously, the average friction coefficient (COFs) of liquid paraffin exhibit the highest friction coefficient of about 0.138. On the contrary, with the introduction of g-C$_3$N$_4$, MoS$_2$ or g-C$_3$N$_4$/MoS$_2$, the COFs were decreased gradually. Especially, the oil sample of 2%-g-C$_3$N$_4$/MoS$_2$ composites show the minimum COFs (~0.08) among all components, which can effectively promote the lubrication effect of base oil, resulted in Fig. 4b. Furthermore, a stable friction curve of 2%-g-C$_3$N$_4$/MoS$_2$ composites with no significant tendency of fluctuation was observed from Fig. 4b inset. Moreover, the tribological experiments of 2%-g-C$_3$N$_4$/MoS$_2$ samples at various applied loads and rotating speeds were also compiled, and resulted in Fig.4. It can be seen that the friction coefficient of all samples show a certain enhancement with the increase of applied loads and rotating speeds. As seen from Fig. 4c, g-C$_3$N$_4$/MoS$_2$ oil samples exhibits lower and more stable friction coefficient than that of liquid paraffin at various applied loads. When the load value increased to 30 N, this oil sample contained with g-C$_3$N$_4$/MoS$_2$ show the lowest COFs of about 0.07. Similarly, with the improvement of rotating speeds from 50 to 500 rpm, the friction coefficientof g-C$_3$N$_4$/MoS$_2$ and liquid paraffin were also first decreased and then increased, and the lowest COFs appeared at 300 rpm(Fig. 4d), which is mainly attributable to the increase of interface temperature and the damage of friction film.
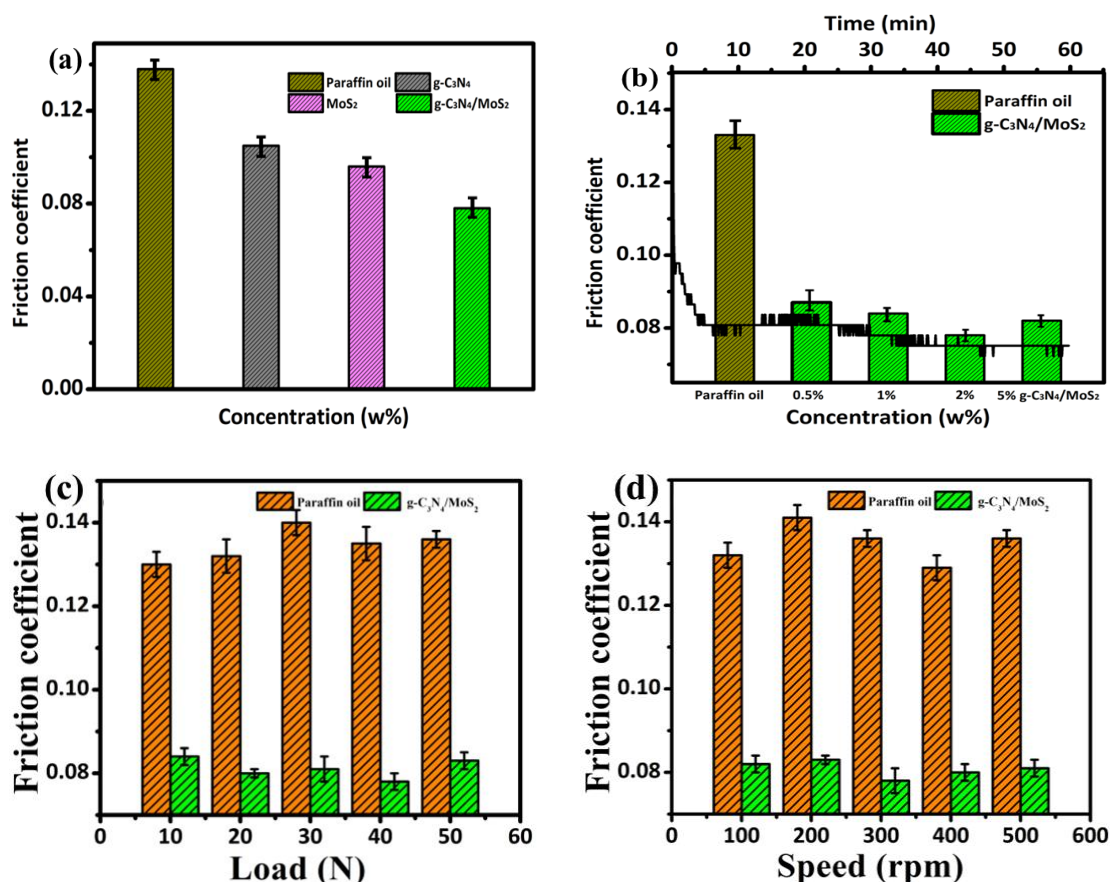
Fig. 4 Friction coefficient curves of the oil, g-C₃N₄, MoS₂,and g-g-C₃N₄/MoS₂ at the speed of 300 r/min(a), Friction coefficient curves of the oil with different g-C₃N₄/MoS₂ contents (0.5wt.% ~ 5.0wt.%) at the speed of 300rpm/min(b),Variations of friction coefficient of lubricant with increasing load (c) and under diverse speeds (d).

The wear scar morphology were perform to investigate the anti-wear property of g-C₃N₄/MoS₂ by SEM and SMP analysis after friction test under an applied load 20 N, sliding velocity of 2 mm/s. According to Fig. 5, the surface of steel disk lubricated by paraffin oil presents the wider wear scar, and worse than that, serious wear (e.g. debris, ploughing and furrow) can be clearly obtained on its surface (Fig. 5a). Nevertheless, when g-C₃N₄/MoS₂ was added in the paraffin oil, the narrower and shallower wear scars were observed (Fig. 5b), and no obvious grinding furrows and cracks appeared, which indicate that composite play a large part in lubrication, significantly reducing the friction and wear between sample disks, achieving the goal of sample protection. Further, the 3D morphologies of wearing surface of steel disk lubricated by liquid paraffin and g-C₃N₄/MoS₂ oil samples were examined SMP technology (Fig.6). As expected, the SMP experiments exhibited the similar to the SEM images of the wear scar, which lubricated by g-C₃N₄/MoS₂ oil samples were relatively smooth, and hardly had large furrows and wrinkle superposition. As lubricated by paraffin oil (Fig. 6a), the maximum wear scar width and depth was approximately 278 μm and 3.7 μm, respectively; while introducing the g-C₃N₄/MoS₂ composites into liquid paraffin, the wear scar width and depth were decreased to 136 μm and 1.5 μm(Fig. 6b). Thus, the existence of 2D/2D g-C₃N₄/MoS₂ efficiently inhibited the deformation of wear surface

and reduced the real contact area, which also provided excellent friction-reducing and anti-wear properties using as a lubricating additive.
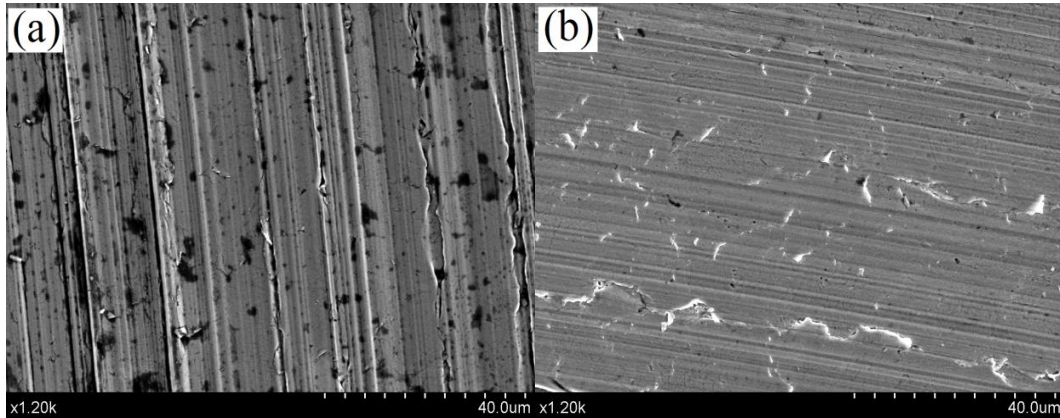

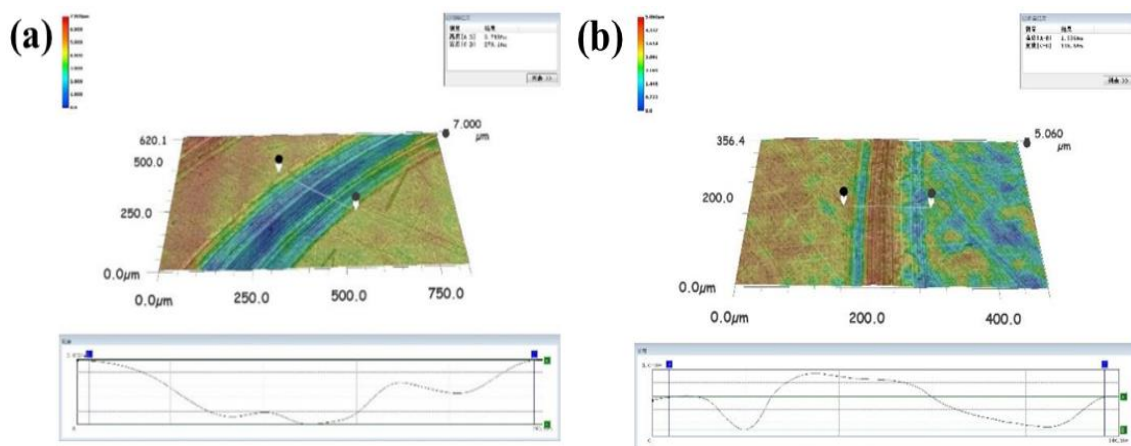Fig. 5. The wear scar of plate: (a) paraffin oil, (b) paraffin oil 2.0 wt.% g-C$_3$N$_4$/MoS$_2$.

Fig. 6. Non-contact optical profile testing instrument images of wear scar: (a) Paraffin oil,
(b) paraffin oil with 2 wt% g-C$_3$N$_4$/MoS$_2$ nanosheets.

Based on analysis mentioned above, a possible lubrication process and tribological mechanism of g-C$_3$N$_4$/MoS$_2$ system was proposed. As we know, the decrease in friction coefficient and wear is mainly owed to rolling effect, mending effect, and the formation of tribo-film. With the friction process proceeding, g-C$_3$N$_4$/MoS$_2$ nanoparticles has a great chance to be adsorbed on interfaces to prevent the friction surface from direct contact and inherit the scar formation. Moreover, the g-C$_3$N$_4$/MoS$_2$ can be easily slid, striped and entered into furrows present in the interfaces because of distinctive layered structure, which can serve as self-lubrication. More importantly, with the addition of g-C$_3$N$_4$/MoS$_2$, a stable and robust tribo-film can be formed under repeated stresses owing to the synergistic effects of lamellar g-C$_3$N$_4$ and MoS$_2$, which not only act as spacer to protect the interfaces of metal-to-metal but also provide the enhancing load carrying and antiwear ability, resulting excellent tribological properties.

4. Conclusions

In summary, the novel 2D/2D g-C$_3$N$_4$/MoS$_2$ heterojunction of MoS$_2$ nanosheets grafted g-C$_3$N$_4$ ultrathin nanosheets were prepared through an in-situ hydrothermal process, which was applied directly as a novel nano-additive in paraffin for the evaluation of lubrication properties. Obviously, all as-prepared g-C$_3$N$_4$/MoS$_2$ composites possessed the obvious reducing-friction and anti-wear properties towards liquid paraffin compared with pure paraffin and the mixture oil samples contained with single g-C$_3$N$_4$ or MoS$_2$. Particularly, 2%-g-C$_3$N$_4$/MoS$_2$-paraffin samples exhibited the optimal tribological properties, which friction coefficient is decreased to 0.08, resulting significantly enhanced reducing-friction and anti-wear properties of liquid paraffin. According to analysis mentioned above, the improvement of tribological property is attributed to the formation of tribofifilm and the synergistic effect between g-C$_3$N$_4$ and MoS$_2$,which will be helpful for the development of additives with nanostructures and possess great application potentials as high performance practical lubricant additives.

References

[1] A. A. F. Mohamed, X. J. Hou, M. Liqiang, ET AL. Wear. 364, 365 (2016). https://doi.org/10.1016/j.wear.2016.07.012

[2] Y. A. Meng, J. L. Sun, J. Q. He, ET AL. Journal of Cleaner Production. 277 (2020).

[3] H. Peng, Q. Wei, Y. Xuan, ET AL. Carbon. 154 (2019). https://doi.org/10.1016/j.carbon.2019.08.010

[4] Rejvani, M., Saedodin, S., Vahedi, S.M. et al. J Therm Anal Calorim 138, 1823–1839 (2019). https://doi.org/10.1007/s10973-019-08225-5

[5] G. Teng, H. L. Chang, Y. Min, ET AL. Journal of Materials Processing Technology. 290 (2021), 116976, https://doi.org/10.1016/j.jmatprotec.2020.116976

[6] P. Huang, A. G. Castellanos, D. Guo, ET AL. Journal of Physical Chemistry C. 122, 47 (2018); https://doi.org/10.1021/acs.jpcc.8b07735

[7] Curry, F. John, Wilson, ET AL. ACS Appl. Mater. Interfaces 2017, 9, 33, 28019–28026. (2018) https://doi.org/10.1021/acsami.7b06917

[8] G. C. Min, B. Alex, P. Alison, ET AL. Surfaces and Interfaces. 26 (2021), 101437. https://doi.org/10.1016/j.surfin.2021.101437

[9] D. D. Ming, C. Yu, Y. L. Rui, ET AL. Extreme Mechanics Letters. 40 (2020), 100988, https://doi.org/10.1016/j.eml.2020.100988

[10] M. Y. Guo, Y. Q. Qing, H. L. Dong, ET AL. Journal of Colloid and Interface Science. 594 (2021).

[11] I. A. Kartsonakis, D. A. Dragatogiannis, E. P. Koumoulos, ET AL. Materials & Design. 102 (2016); https://doi.org/10.1016/j.matdes.2016.04.027

[12] Hui Xie, Yajuan Zhao,, ET AL. Carbon. 152 (2019) p. 295 https://doi.org/10.1016/j.carbon.2019.06.029

[13] L. Zhang, J. Pu, L. Wang, ET AL. Acs Appl Mater Interfaces. 7, 16 (2015); https://doi.org/10.1021/acsami.5b00598

[14] J. Bao, Z. Jun, Y. C. Guang, ET AL. Applied Surface Science. 546 (2021).

[15] M. José, D. R. Liñeira, J. G. María, ET AL. Journal of Molecular Liquids. 345 (2022).

[16] R. Y. Mei, X. Q. Jia, H. X. Wen, ET AL. Tribology International. 167 (2022).

[17] C. M. Kalyan, Y. M. A. Wu, E. Ali, ET AL. Carbon. 146 (2019).

[18] B. Khac, K. H. Chung, ET AL. J Nanosci Nanotechnol. 16, 5 (2016); https://doi.org/10.1166/jnn.2016.11004

[19] X. Zhu, X. Wei, Y. Huang, ET AL. Metals. 9, 3 (2019); https://doi.org/10.3390/met9030356

[20] Yiming Song, Jin Wang, Yiran Wang, Michael Urbakh, Quanshui Zheng, and Ming Ma, Phys. Rev. Materials 5, 084002, https://doi.org/10.1103/PhysRevMaterials.5.084002

[21] Q. L. Xiu, Z. W. Shi, X. Y. Qing, ET AL. Ceramics International. 46 (2020).

[22] I. Tudela, A. J. Cobley, Y. Zhang, ET AL. Friction. 7, 02 (2019); https://doi.org/10.1007/s40544-018-0211-0

[23] F. Pragati, K. Y. Sudharshan, N. Roshan, ET AL. Electrochimica Acta. 258 (2017).

[24] J. W. Ze, L. J. Zhi, R. W. Guo, ET AL. International Journal of Hydrogen Energy. 43, 29 (2018).

[25] D. Ky, B. T. Khac, C. T. Le, ET AL. Friction. (2017).

[26] B. C. Bei, L. Xiang, H. J. Yu, ET AL. Applied Science and Manufacturing. 109 (2018), Pages 232-238, https://doi.org/10.1016/j.compositesa.2018.02.039